Becker-Kerber, B., Abd Elmola, A., Zhuravlev, A., Gaucher, C., Simões, M.G., Prado, G.M.E.M., Gámez Vintaned, J.A., Fontaine, C., Lino, L.M., Ferreira Sanchez, D., Galante, D., Paim, P.S.G., Callefo, F., Kerber, G., Meunier, A., and El Albani, A., 2021, Clay templates in Ediacaran vendotaeniaceans: Implications for the taphonomy of carbonaceous fossils: GSA Bulletin, https://doi.org/10.1130/B36033.1.

Supplemental Material

Table A1. Normalized chemical analyses (oxides weight %) of the clay minerals observed in the samples and the corresponding calculated structural formulae plotted in binary/ternary diagrams.

Fig. S1. Sobramil locality, former Itaú quarry (19°0'3.80"S – 57°37'12.70"O). (A) Satellite image of the area. (B) Schematic drawing showing the position of the studied sections (A, B, and C), and the dip angle and dip directions measured at some rock layer surfaces.

Fig. S2. Sections at the Sobramil locality. (A) Section A and its schematic drawing showing the approximate fossil-bearing levels analyzed in this study. Abundant remains of *Corumbella* occur at the middle-top of the fine-grained siliciclastic level 1. Putative trace fossils are very common between *Corumbella* levels. Rare *Vendotaenia* fossils were observed at the base of the exposed siliciclastic beds. (B) Section B, schematic drawing with the stratigraphic position of the fossil occurrences. Rare *Cloudina* fragments were found at the base of section B, but the most abundant concentrations of this Ediacaran guide-fossil are recorded at the top of the section. No *Corumbella* remains were found in the mudstone/siltstone level 2, but a high density of putative tubular trace fossils is observed.

Fig. S3. Section C at the Sobramil locality. (A) Field image of the local weathered rock exposure. (B) Schematic drawing with the *Vendotaenia*-bearing level highlighted. *Corumbella* remains are not so common in this siliciclastic level. Hammer for scale.

Fig. S4. XRD results of the bulk and clay-fractions. (A) X-ray diffraction traces (random powder preparations) of some representative bulk powder samples. (B) X-ray diffraction traces (oriented preparations) of the <2 μm size-fraction; black-colored patterns refer to untreated samples under air-drying conditions, whereas the ethylene glycol saturated samples are represented by the red-colored patterns. S= smectite; I = illite; Chl-S= chlorite-smectite mixed layers; Ca=calcite; Q= quartz.

Fig. S5. XRD results of the clay-fraction (random powder preparations) of the fossil (A) and host rock (B), respectively, showing the d_{060} region of clay minerals.

Fig. S6. Mid-infrared patterns (clay fractions) of the samples showing clear differences between fossil and host rock (at different levels).

Fig. S7. Near-infrared patterns (clay fractions) of the samples showing differences between fossil and host rock (at different levels).

Fig. S8. EDS and SR-μXRF elemental composition of *Vendotaenia*. (A) Composite EDS map of the rock-bedding plane with the fossil. (B–G) Elemental maps of sample (A). (H–M) SR-μXRF

maps of a cross-section of *Vendotaenia* (ellipsoidal structure at the top of the figures) showing principal differences of the fossil and matrix composition.

Fig. S9. SR-μXRF 2D map of a *Vendotaenia* cross-section (middle of the figure) associated with fibrous minerals (arrow), showing the distribution of Si (A), K (B), Mn (C), Ca (D), Fe (E), Cu (F), Al (G). (H) Polished section perpendicular to the long axis of *Vendotaenia* and parallel to the orientation of the fibers (arrow) showing the mapped region (black rectangle).

Fig. S10. EDS mapping of the host rock (mudstones) polished sections. (A–B) Mix image showing the main elemental composition of the sedimentary framework and matrix of the siliciclastic levels. Electron image (A1, B1) and elemental maps of Al (A2, B2), K (A3, B3), Si (A4, B4), Mg (A5, B5), and Fe (A6, B6).

Fig. S11. EDS mapping of polished sections of carbonates from the Sobramil quarry. (A) A mix of elemental maps of Al, Si, and Ca. Individual elemental maps showing the distribution of Si (B), Al (C), Mg (D), K (E), Fe (F), and Ca (G).

SUPPLEMENTARY FIGURES

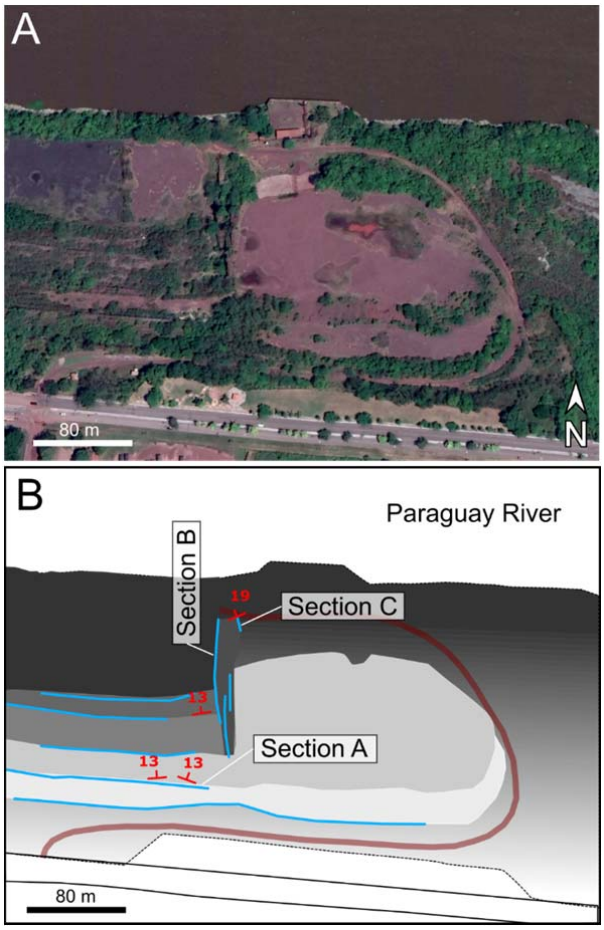

Fig. S1. Sobramil locality, former Itaú quarry (**19°0'3.80"S – 57°37'12.70"O**). (A) Satellite image of the area. (B) Schematic drawing showing the position of the studied sections (A, B, and C), and the dip angle and dip directions measured at some rock layer surfaces.

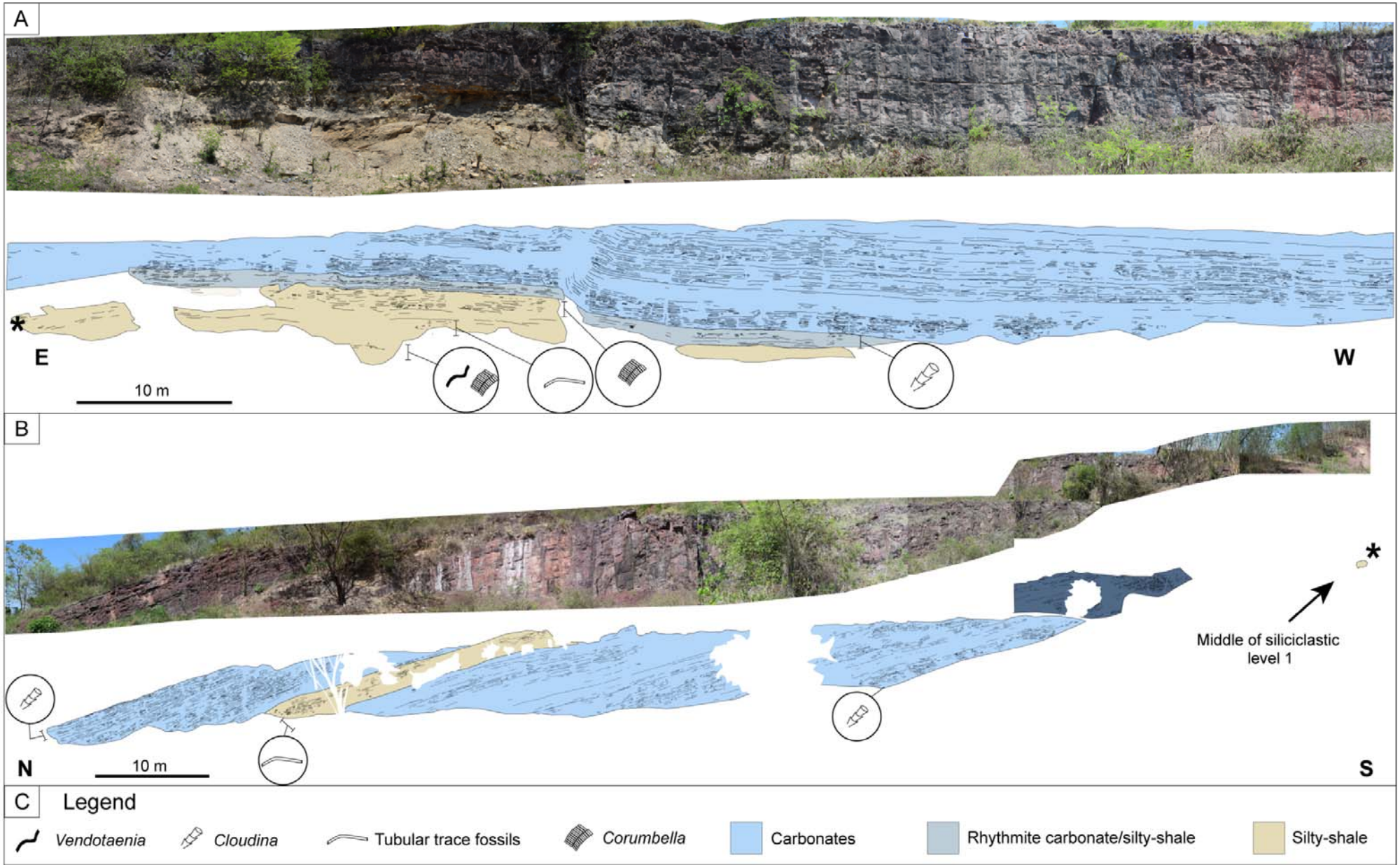
A
E
W
10 m
B
N
S
10 m
Middle of siliciclastic level 1
C
Legend
Vendotaenia
Cloudina
Tubular trace fossils
Corumbella
Carbonates
Rhythmite carbonate/silty-shale
Silty-shale

Fig. S2. Sections at the Sobramil locality. (A) Section A and its schematic drawing showing the approximate fossil-bearing levels analyzed in this study. Abundant remains of *Corumbella* occur at the middle-top of the fine-grained siliciclastic level 1. Putative trace fossils are very common between *Corumbella* levels. Rare *Vendotaenia* fossils were observed at the base of the exposed siliciclastic beds. (B) Section B, schematic drawing with the stratigraphic position of the fossil occurrences. Rare *Cloudina* fragments were found at the base of section B, but the most abundant concentrations of this Ediacaran guide-fossil are recorded at the top of the section. No *Corumbella* remains were found in the mudstone/siltstone level 2, but a high density of putative tubular trace fossils is observed.

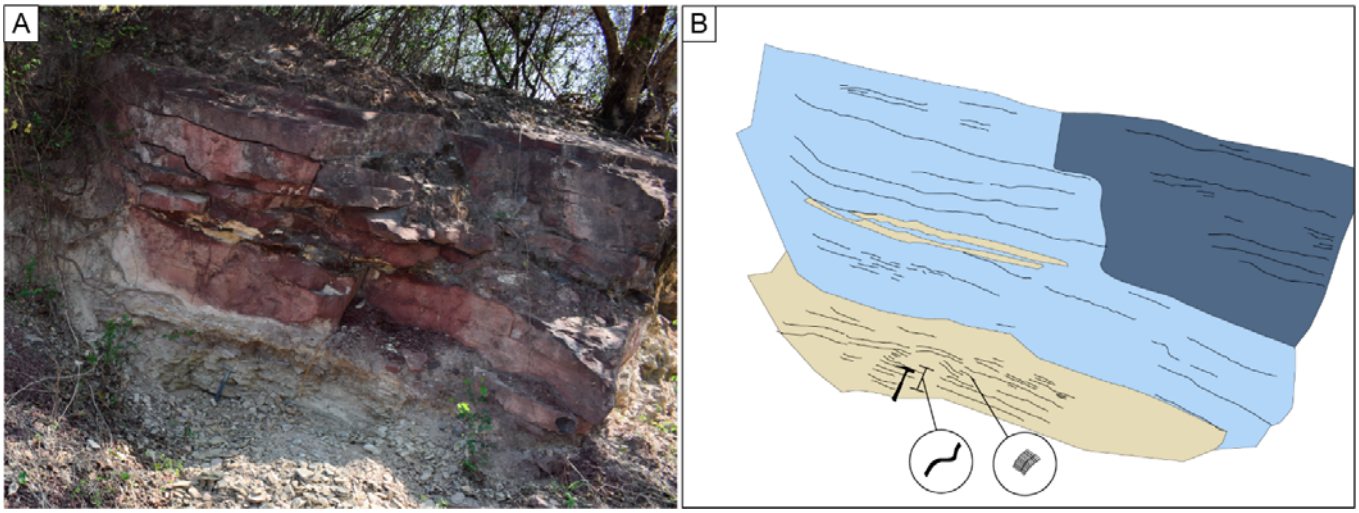

Fig. S3. Section C at the Sobramil locality. (A) Field image of the local weathered rock exposure. (B) Schematic drawing with the *Vendotaenia*-bearing level highlighted. *Corumbella* remains are not so common in this siliciclastic level. Hammer for scale.

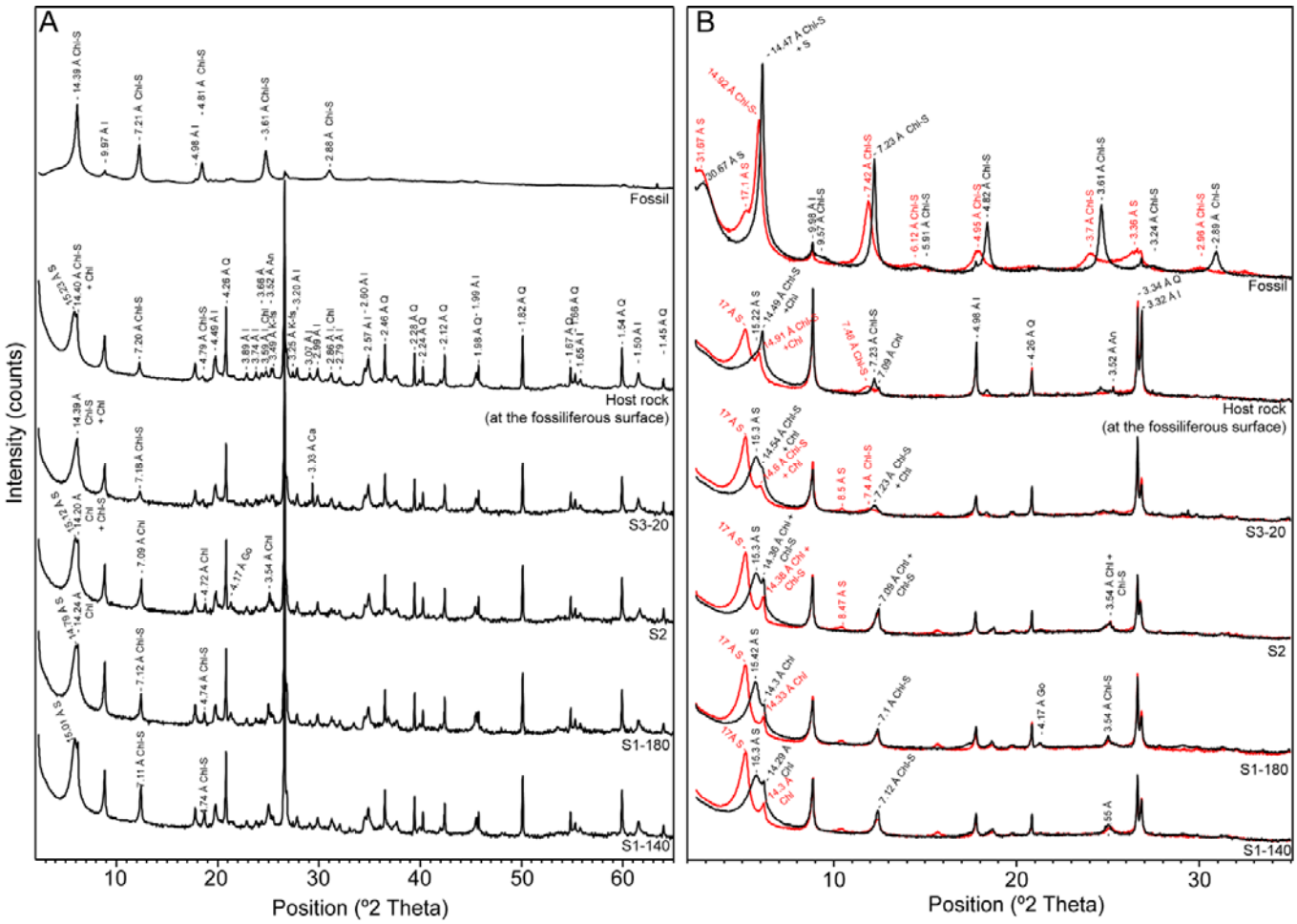

Fig. S4. XRD results of the bulk and clay-fractions. (A) X-ray diffraction traces (random powder preparations) of some representative bulk powder samples. (B) X-ray diffraction traces (oriented preparations) of the <2 μm size-fraction; black-colored patterns refer to untreated samples under air-drying conditions, whereas the ethylene glycol saturated samples are represented by the red-colored patterns. S= smectite; I = illite; Chl-S= chlorite-smectite mixed layers; Ca=calcite; Q= quartz.

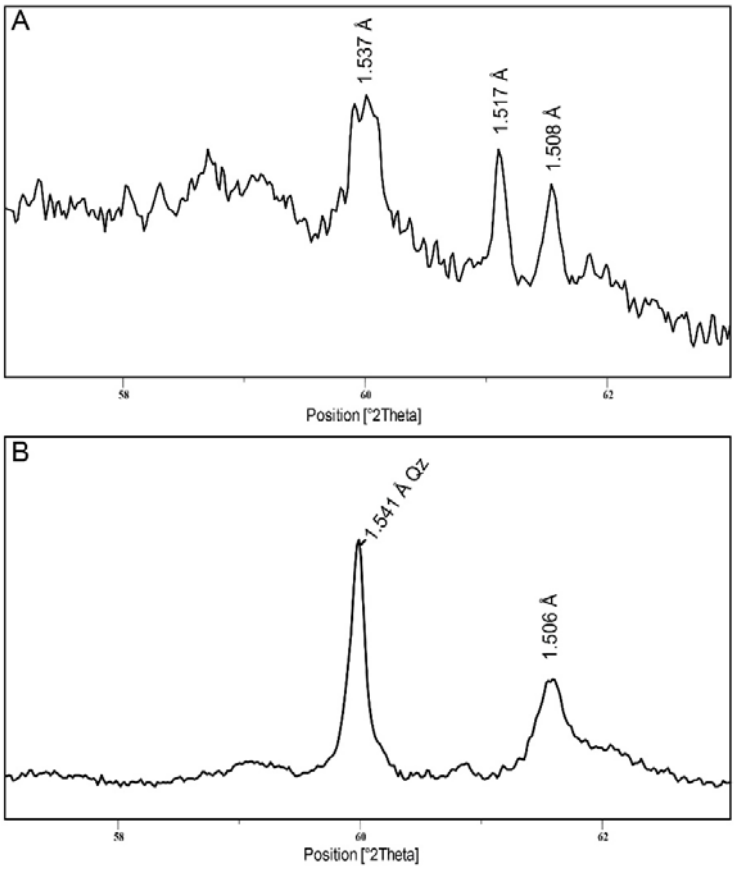

Fig. S5. XRD results of the clay-fraction (random powder preparations) of the fossil (A) and host rock (B), respectively, showing the d_{060} region of clay minerals.

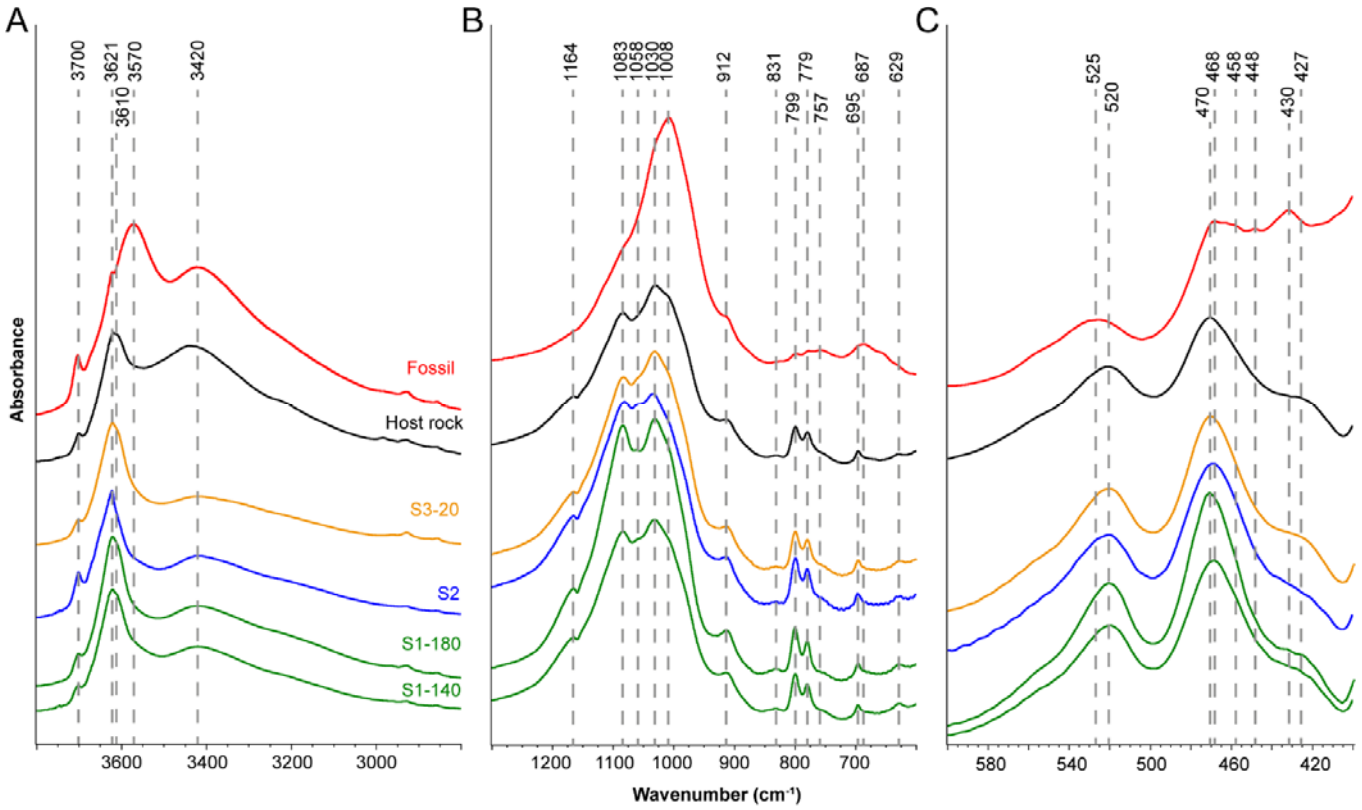

Fig. S6. Mid-infrared patterns (clay fractions) of the samples showing clear differences between fossil and host rock (at different levels).

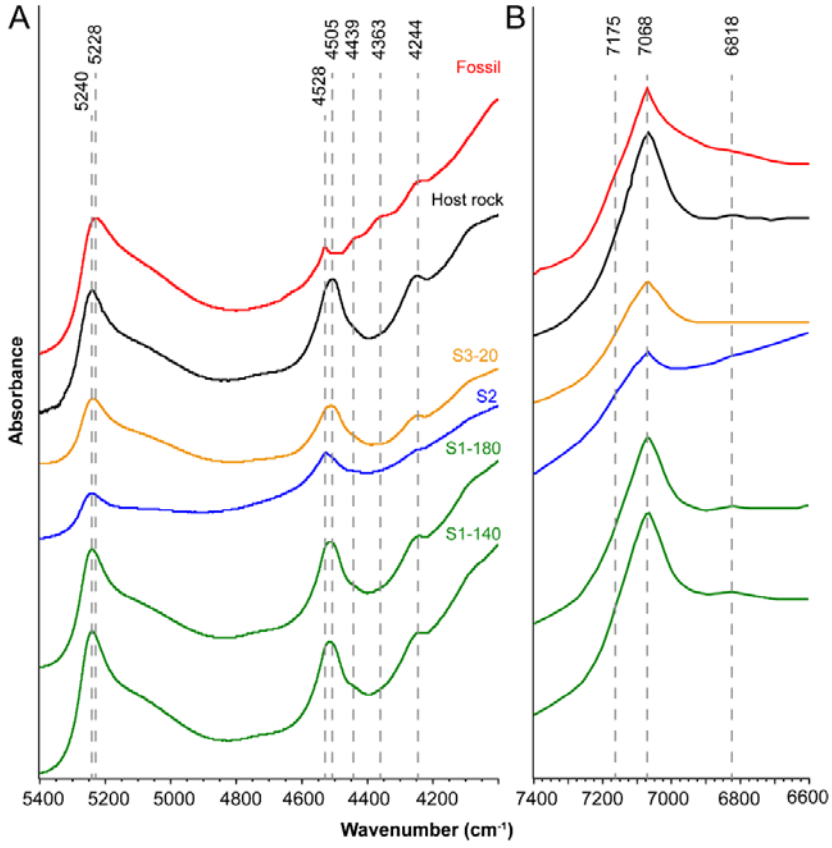

Fig. S7. Near-infrared patterns (clay fractions) of the samples showing differences between fossil and host rock (at different levels).

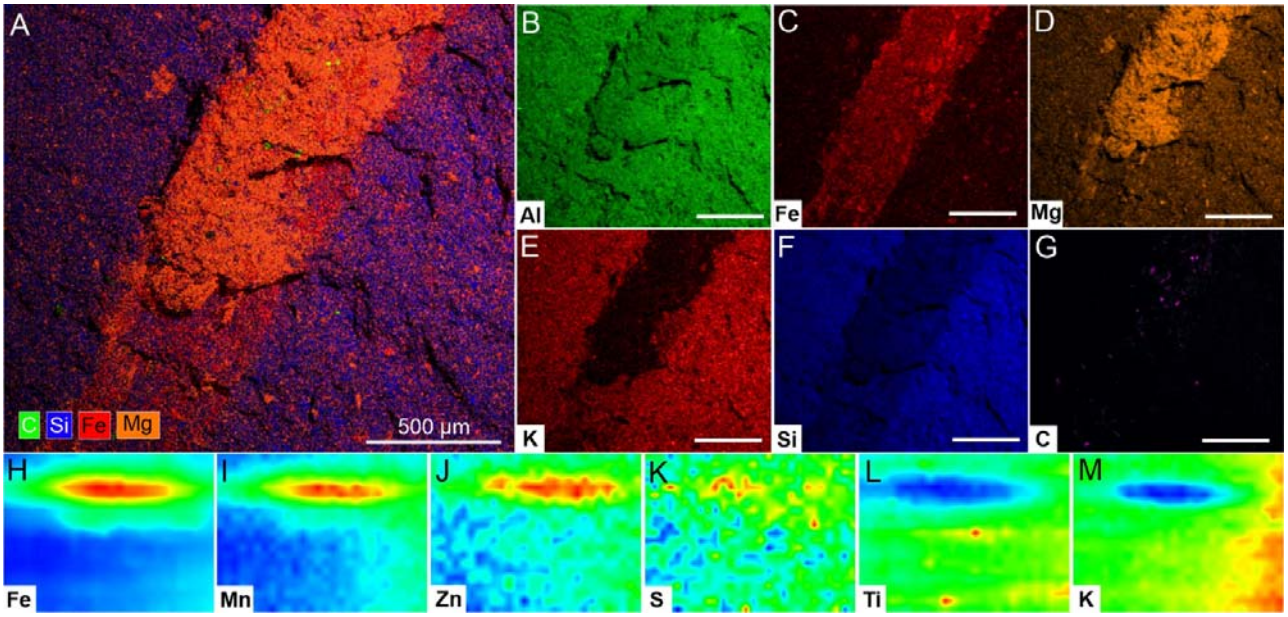

Fig. S8. EDS and SR-µXRF elemental composition of *Vendotaenia*. (A) Composite EDS map of the rock-bedding plane with the fossil. (B–G) Elemental maps of sample (A). (H–M) SR-µXRF maps of a cross-section of *Vendotaenia* (ellipsoidal structure at the top of the figures) showing principal differences of the fossil and matrix composition.

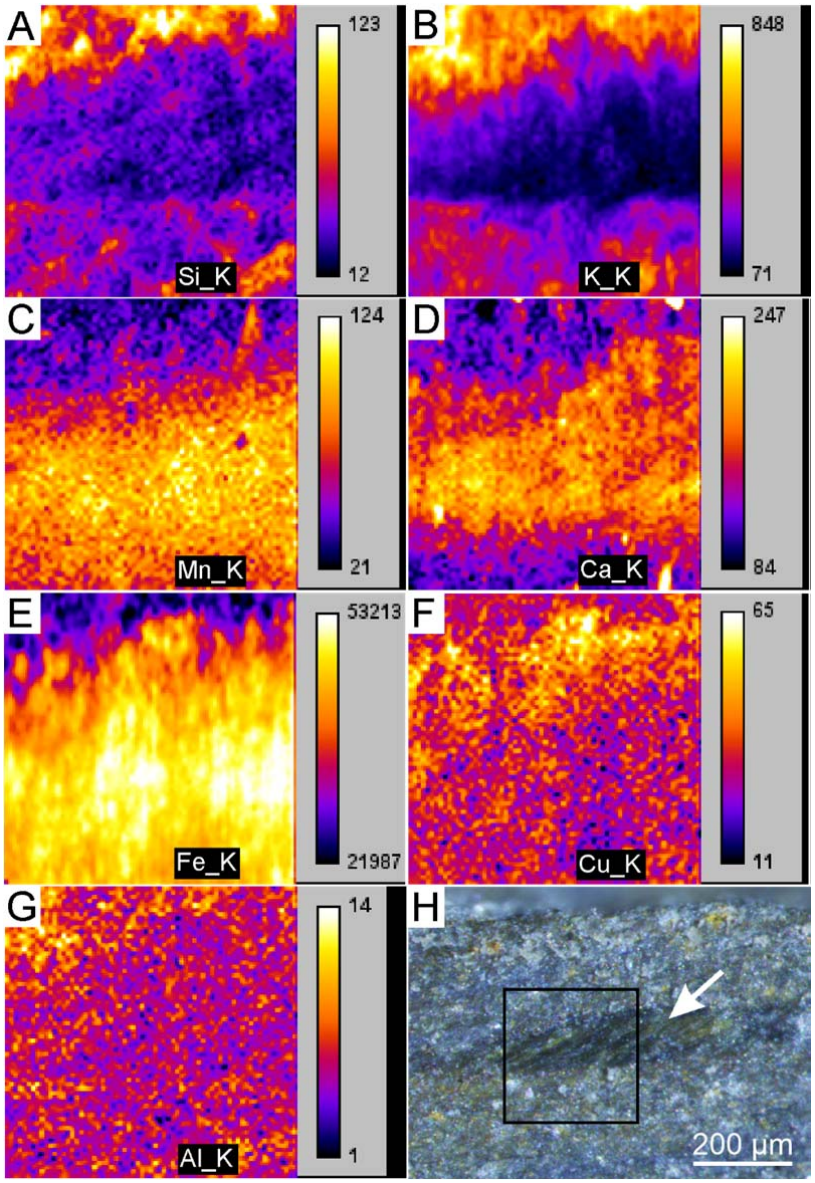

Fig. S9. SR-µXRF 2D map of a *Vendotaenia* cross-section (middle of the figure) associated with fibrous minerals (arrow), showing the distribution of Si (A), K (B), Mn (C), Ca (D), Fe (E), Cu (F), Al (G). (H) Polished section perpendicular to the long axis of *Vendotaenia* and parallel to the orientation of the fibers (arrow) showing the mapped region (black rectangle).

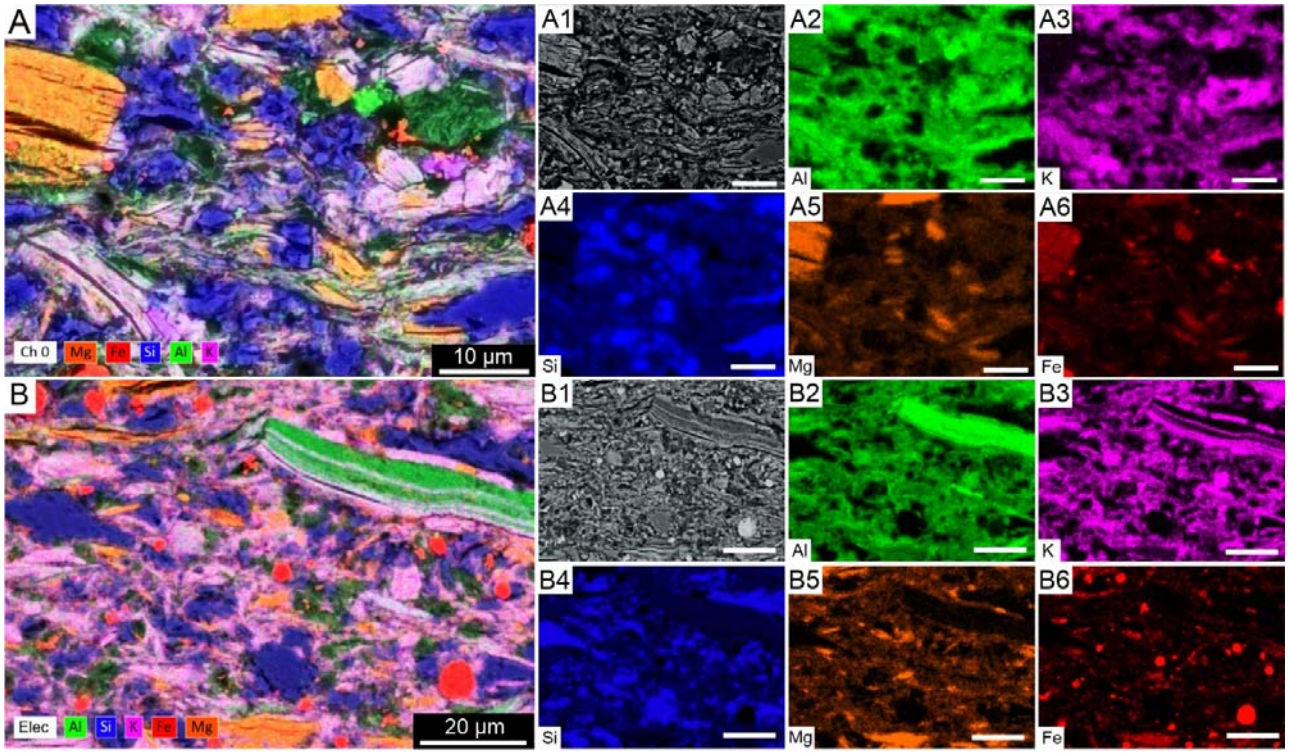

Fig. S10. EDS mapping of the host rock (mudstones) polished sections. (A–B) Mix image showing the main elemental composition of the sedimentary framework and matrix of the siliciclastic levels. Electron image (A1, B1) and elemental maps of Al (A2, B2), K (A3, B3), Si (A4, B4), Mg (A5, B5), and Fe (A6, B6).

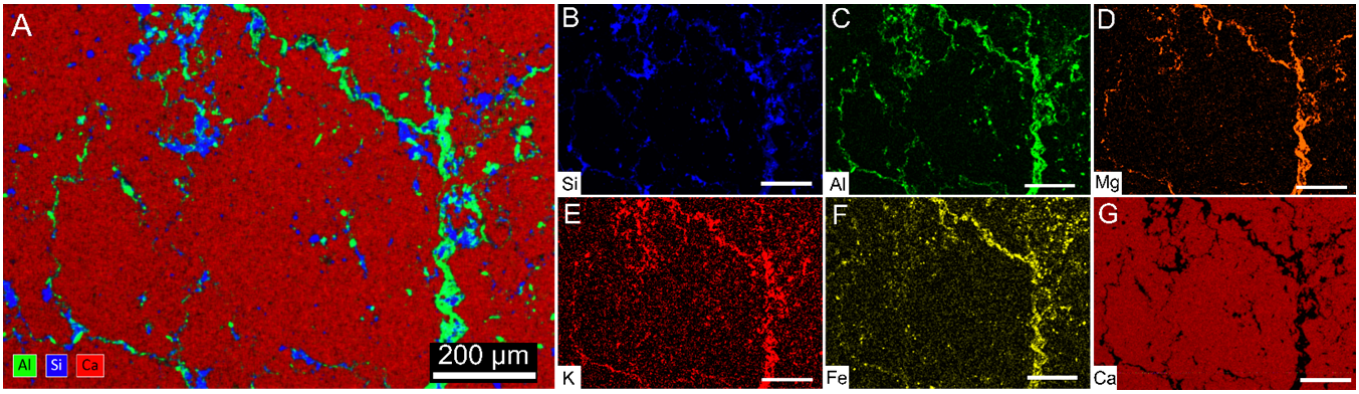

Fig. S11. EDS mapping of polished sections of carbonates from the Sobramil quarry. (A) A mix of elemental maps of Al, Si, and Ca. Individual elemental maps showing the distribution of Si (B), Al (C), Mg (D), K (E), Fe (F), and Ca (G).